$Me_5C_5Ni(acac)$: A Monomeric, Paramagnetic, 18-Electron, Spin-Equilibrium Molecule

Michael E. Smith and Richard A. Andersen*

Contribution from the Chemistry Department and Chemical Sciences Division of Lawrence Berkeley Laboratory, University of California, Berkeley, California 94720

Received November 15, 1995. Revised Manuscript Received May 21, 1996[⊗]

Abstract: New synthetic procedures have been developed for $Me_5C_5M(acac)$, M = Co or Ni. The crystal structures of these 17- or 18-electron monomers show that the compounds are isomorphous and in space group $P\bar{1}$, with the planes defined by the Me_5C_5 ring and the M(acac) fragment perpendicular to within 5°. The Me_5C_5 ring in both molecules has an ene−allyl distortion which is rationalized by the low molecular symmetry (C_s), which removes the degeneracy in the e^+ and e^- ring orbitals. The electronic structure of the cobalt compound is ^2A, as deduced from magnetic susceptibility and EPR spectroscopy. The electronic structure of the nickel compound depends upon the temperature. In the solid state, the compound is diamagnetic below 150 K, but it becomes paramagnetic with increasing temperature. The ^1H NMR chemical shifts of the compound in solution are nonlinear in temperature, and a plot of δ vs T^{-1} yields an equilibrium constant of 0.47 at 303 K for the low spin ↔ high spin equilibrium. The 20-electron phosphine complexes of nickel can be isolated; $Me_5C_5Ni(acac)(PMe_3)$ is a simple paramagnet with two unpaired spins, but the PEt_3 complex exists in equilibrium with its base-free compound in solution. The cobalt compound does not give an isolable phosphine complex. A simple symmetry orbital model is proposed that accounts for the electronic and molecular structures of these organometallic compounds.

Introduction

The d-transition-metal acetylacetonate compounds were used extensively as starting materials in the early days of metallocene chemistry,[1] presumably due to their ease of preparation and solubility in ethereal solvents.[2] They have been used sporadically in the synthesis of Me_5C_5 compounds. The rhodium cation, $[(Me_5C_5)_2Rh_2(acac)_2](BF_4)_2$, and the ruthenium neutral species, $(Me_5C_5)_2Ru_2(acac)_2$, are interesting since both of these d^6-metal centers achieve an 18-electron configuration in rather unusual ways. The acetylacetonate ligand is bidentate (using the oxygen atoms) toward the metal center, the metal atom is sitting on the pseudo-C_5 axis of the Me_5C_5 group, and the acac group is tilted relative to the ring centroid by *ca.* 30°.[3] If monomeric, both compounds would be highly unusual examples of 16-electron compounds; indeed the original publication of "$(Me_5C_5)Ru(acac)$" makes such a claim.[3c] Both compounds, however, avoid electronic unsaturation by forming a dimer with the γ-carbon atom of the acac acting as a two-electron donor to the adjacent metal center. Thus, the acac ligand is a five-electron ligand in these compounds. The only 3d-metal cyclopentadienyl acetylacetonates that have been described are $Me_5C_5M(acac)$, where M = Co (17 e) and Ni (18 e).[4] These molecules are monomeric in the gas phase, but their molecular and electronic structures are unknown. We have recently discovered that these two compounds are excellent starting materials for the synthesis of $(Me_5C_5)_3M_3(\mu_3\text{-CH})(\mu\text{-H})$ clusters.[5] In this paper we show that the solid state molecular structure of these compounds has distorted Me_5C_5 rings, the reason for which is the presence of one (M = Co) or two (M = Ni) electrons in a Me_5C_5−M ring antibonding orbital, and that the electronic structure in the solid state and in solution are consistent with this postulate.

Results

Synthesis. Our synthetic reactions are a little different than those described in preliminary form by Manriquez.[4] Use of soluble $(Me_5C_5)_2Mg$[6] rather than insoluble Me_5C_5Li gives yields of $Me_5C_5M(acac)$ in excess of 80%. Both compounds are red, melt at *ca.* 100 °C, and are soluble in aromatic and ethereal solvents. They sublime under reduced pressure at *ca.* 60 °C, and they give monomeric molecular ions in their mass spectra. In the solid state the infrared spectra are superimposable; the absorptions for the nickel compound are a few (5−15) wavenumbers higher, and they are isomorphous by X-ray crystallography.

Molecular Structure. The crystal structures of both compounds were determined, and an ORTEP diagram is shown for the cobalt compound in Figure 1; the nickel compound is isomorphous. Both crystallized in space group $P\bar{1}$ (No. 2) with two independent molecules in the asymmetric unit, and the numbering schemes are identical. The distance between the metal in one independent molecule and the γ-carbon atom of the acetylacetonate in the adjacent molecule is greater than 3.5 Å. Selected bond distances and angles are given in Tables 1 and 2, and crystal data are in Table 3. A complete listing of bond distances, angles, anisotropic thermal parameters, and positional parameters is available as Supporting Information.

The molecules are derived by the interaction of the two fragments, Me_5C_5 and M(acac); the least squares planes defined by the Me_5C_5 ligand and the M(acac) fragment are all within 5.5° of perpendicular for a given molecule. The M−O distances

* Address correspondence to this author at Chemistry Department, University of California, Berkeley, CA 94720.

[⊗] Abstract published in *Advance ACS Abstracts,* November 1, 1996.

(1) Wilkinson, G.; Cotton, F. A. *Prog. Inorg. Chem.* **1959**, *1*, 1.

(2) Fackler, J. P. *Prog. Inorg. Chem.* **1966**, *7*, 361.

(3) (a) Rigby, N.; Lee, H. B.; Bailey, P. M.; McCleverty, J. A.; Maitles, P. M. *J. Chem. Soc., Dalton Trans.* **1979**, 387. (b) Smith, M. E.; Hollander, F. J.; Andersen, R. A. *Angew. Chem., Int. Ed. Engl.* **1993**, *32*, 1294. (c) Kölle, U.; Kossakowski, J.; Raabe, G. *Angew. Chem., Int. Ed. Engl.* **1990**, *29*, 773.

(4) (a) Bunel, E. E.; Valle, L.; Manriquez, J. M. *Organometallics* **1985**, *4*, 1680. (b) The Me_5C_5 ring in $Me_5C_5Co(acac)$, cocrystallized with C_6F_5, is said to be pentahapto-bound though no C−C distances are given and the Co−C distances range from 2.09 to 2.03 Å. Schneider, J. J.; Goddard, R.; Krüger, K. *Z. Naturforsch.* **1995**, *50b*, 448.

(5) Smith, M. E.; Andersen, R. A. *Organometallics* **1996**, *15*, 2680.

(6) Andersen, R. A.; Blom, R.; Boncella, J. M.; Burns, C. J.; Volden, H. V. *Acta Chem. Scand.* **1987**, *A41*, 24.

S0002-7863(95)03873-X CCC: $12.00

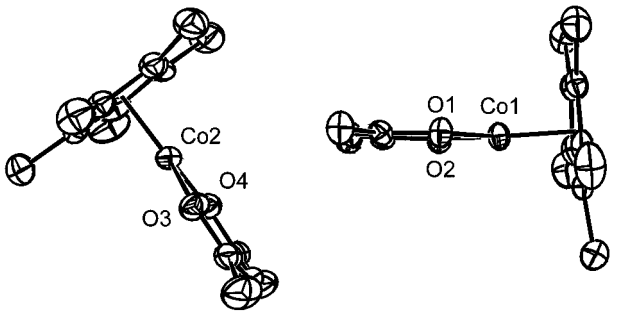

Figure 1. ORTEP diagram for $(Me_5C_5)Co(acac)$ showing the two molecules in the asymmetric unit cell, the ellipsoids represent 50% probability values. The nickel compound is isomorphous so no diagram is shown; the numbering scheme is identical for both molecules.

Table 1. Bond Distances for $(Me_5C_5)M(acac)$ in Å

	(a) M = Co		
Co1−O1	1.883 (3)	O1−C2	1.278 (5)
Co1−O2	1.887 (3)	O2−C4	1.283 (5)
Co2−O3	1.876 (3)	O3−C22	1.276 (6)
Co2−O4	1.872 (3)	O4−C24	1.284 (6)
Co−O (av)	1.880 (2)	O−C (av)	1.280 (3)
Co1−C6	2.066 (5)	C6−C7	1.423 (7)
Co1−C7	2.118 (4)	C7−C8	1.412 (7)
Co1−C8	2.054 (4)	C8−C9	1.444 (7)
Co1−C9	2.091 (4)	C9−C10	1.398 (6)
Co1−C10	2.085 (5)	C6−C10	1.425 (7)
Co2−C26	2.093 (5)	C26−C27	1.419 (7)
Co2−C27	2.088 (5)	C27−C28	1.431 (7)
Co2−C28	2.050 (5)	C28−C29	1.407 (7)
Co2−C29	2.092 (5)	C29−C30	1.431 (7)
Co2−C30	2.052 (5)	C26−C30	1.412 (7)
Co−C_a (av)	2.105 (3)	C_a−C_b (av)	1.418 (4)
Co−C_b (av)	2.056 (2)	C_b−C_c (av)	1.428 (4)
Co−C_c (av)	2.089 (2)	C_c−C_c (av)	1.409 (5)
Co1−Cp1	1.70	Co−Cp (av)	1.69
Co2−Cp2	1.69		
	(b) M = Ni		
Ni1−O1	1.890 (4)	O1−C2	1.280 (5)
Ni1−O2	1.883 (3)	O2−C4	1.282 (6)
Ni2−O3	1.868 (4)	O3−C22	1.290 (5)
Ni2−O4	1.876 (4)	O4−C24	1.294 (5)
Ni−O (av)	1.879 (2)	O−C (av)	1.287 (3)
Ni1−C6	2.074 (5)	C6−C7	1.432 (8)
Ni1−C7	2.143 (4)	C7−C8	1.417 (9)
Ni1−C8	2.074 (5)	C8−C9	1.474 (6)
Ni1−C9	2.196 (5)	C9−C10	1.382 (9)
Ni1−C10	2.188 (5)	C6−C10	1.460 (8)
Ni2−C26	2.183 (5)	C26−C27	1.361 (9)
Ni2−C27	2.200 (5)	C27−C28	1.467 (7)
Ni2−C28	2.062 (5)	C28−C29	1.423 (10)
Ni2−C29	2.123 (4)	C29−C30	1.409 (8)
Ni2−C30	2.060 (5)	C26−C30	1.465 (8)
Ni−C_a (av)	2.133 (3)	C_a−C_b (av)	1.420 (4)
Ni−C_b (av)	2.068 (3)	C_b−C_c (av)	1.467 (4)
Ni−C_c (av)	2.192 (3)	C_c−C_c (av)	1.372 (6)
Ni1−Cp1	1.75	Ni−Cp (av)	1.75
Ni2−Cp2	1.75		

are identical, and the O−M−O and O−M−centroid angles are nearly so. The principal difference between the two compounds is the extent to which the M(acac) fragment is slipped off the pseudo-C_5 axis of the Me_5C_5 ring; the displacement is greater in the nickel compound than in the cobalt one. This can be seen, in general, by the spread in M−C(av) distances, which for cobalt range from 2.056 (2) to 2.105 (3) Å, while for nickel the range is from 2.068 (3) to 2.192 (3) Å. The displacement can be seen readily in Figure 2, which shows the view down the planar Ni(acac) fragment and emphasizes the relationship to four-coordinate nickel(II). The Me_5C_5 ring is closer to cobalt than nickel, and this is shown by the M ring−centroid distances

Table 2. Bond Angles for $(Me_5C_5)M(acac)$ in deg[a]

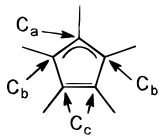

	(a) M = Co		
O1−Co1−O2	95.3(1)	C7−C6−C10	108.8(4)
O3−Co1−O4	95.4(1)	C6−C7−C8	106.6(4)
		C7−C8−C9	108.8(4)
O−Co−O (av)	95.3(1)	C8−C9−C10	107.2(4)
		C6−C10−C9	108.3(4)
Cp1−Co1−O1	133	C27−C26−C30	107.7(4)
Cp1−Co1−O2	131	C26−C27−C28	107.2(4)
Cp2−Co2−O3	132	C27−C28−C29	109.3(4)
Cp2−Co2−O4	133	C28−C29−C30	106.4(4)
		C26−C30−C29	109.2(4)
Cp−Co−O (av)	132		
		C_b−C_a−C_b (av)	106.5(3)
		C_a−C_b−C_c (av)	109.0(2)
		C_b−C_c−C_c (av)	107.6(2)
	(b) M = Ni		
O1−Ni1−O2	98.0(2)	C7−C6−C10	108.6(5)
O3−Ni2−O4	98.7(2)	C6−C7−C8	106.3(4)
		C7−C8−C9	108.6(5)
O−Ni−O (av)	98.3(1)	C8−C9−C10	107.6(5)
		C6−C10−C9	108.0(4)
Cp1−Ni1−O1	131	C27−C26−C30	108.2(5)
Cp1−Ni1−O2	130	C26−C27−C28	107.5(5)
Cp2−Ni2−O3	130	C27−C28−C29	108.7(5)
Cp2−Ni2−O4	131	C28−C29−C30	105.8(5)
		C26−C30−C29	108.9(6)
Cp−Ni−O (av)	131		
		C_b−C_a−C_b (av)	106.1(3)
		C_a−C_b−C_c (av)	108.7(3)
		C_b−C_c−C_c (av)	107.8(2)

[a] Cp1 and Cp2 are the ring centroids of atoms C6−C10 and C26−C30, respectively. C_a, C_b, and C_c refer to the three unique carbon positions in the Cp ene−allyl distortion; see figure.

of 1.70 Å for cobalt and 1.75 Å for nickel. The larger spread in Ni−C distances relative to the Co−C ones is also observed in the C−C distances in the Me_5C_5 ring for each compound. For cobalt, the averaged C_a−C_b distance is 1.418 (4) Å, the C_b−C_c distance is 1.428 (4) Å, and the C_c−C_c distance is 1.409 (5) Å, while for nickel the distances are 1.420 (4), 1.467 (4), and 1.372 (6) Å, respectively. The pattern in the C−C distances is indicative of an ene−allyl distortion. Close inspection of the dihedral angle (ω) formed by the intersection of the least squares planes containing the ene and allyl portions of the Me_5C_5 ligand also shows a subtle difference in the two compounds, *viz.*, ω is larger for the nickel compound. These and other distortion parameters are listed in Table 4.

Electronic Structure. Magnetic Susceptibility. A plot of $(\chi_M)^{-1}$ as a function of absolute temperature for $Me_5C_5Co(acac)$ is shown in Figure 3a. The cobalt compound obeys the Curie−Weiss law with $\mu_{eff} = 1.94\ \mu_B$ and $\theta = -8.7$ K at 5 kG and $\mu_{eff} = 1.91\ \mu_B$ and $\theta = -6.5$ K at 40 kG. In solution, the magnetic moment is 1.9 μ_B at 303 K in C_6D_6. In methylcyclohexane solution, the cobalt compound shows an isotropic eight-line EPR spectrum (^{59}Co, $I = {}^7/_2$), with $g_{iso} = 2.099$ and $A_{iso} = 45.17$ G. A rhombic spectrum is observed on a frozen glass at 2 K with $g_1 = 1.970$, $A_1 = 43.11$ G; $g_2 = 2.091$, A_2 is small; and $g_3 = 2.241$, $A_3 = 105.47$ G. The cobalt compound is well-behaved magnetically; it has one unpaired electron with a magnetic moment and a g value that indicate that the orbital angular momentum is not completely quenched and that the ground state is of low symmetry.

Table 3. Selected Crystal Data for $(Me_5C_5)Co(acac)$, $(Me_5C_5)Ni(acac)$, and $(Me_5C_5)Ni(acac)(PMe_3)$

formula	$CoO_2C_{15}H_{22}$	$NiO_2C_{15}H_{22}$	$NiPO_2C_{18}H_{31}$
FW	293.27	293.05	369.13
space group	$P\bar{1}$ (No. 2)	$P\bar{1}$ (No. 2)	*Pnma* (No. 62)
a, Å	8.539 (3)	8.4857 (20)	13.3111 (30)
b, Å	12.399 (4)	12.4969 (32)	13.8551 (17)
c, Å	15.505 (4)	15.9013 (25)	10.6376 (34)
α, deg	70.39 (2)	68.608 (17)	
β, deg	81.04 (2)	77.179 (16)	
γ, deg	72.64 (2)	71.958 (21)	
V, Å^3	1473.1 (6)	1481.5 (6)	1961.9 (8)
Z	4	4	4
F(000)	620	624	792
d_{calc}, g/cm^3	1.322	1.314	1.250
μ_{calc}, cm^{-1}	11.54	13.06	10.77
size, mm	0.50 × 0.39 × 0.20	0.50 × 0.42 × 0.25	0.20 × 0.27 × 0.34
temperature, °C	−110	−103	−125
diffractometer	Enraf-Nonius CAD4		
radiation	Mo Kα (0.710 73 Å)		
monochromator	highly oriented graphite		
scan range, type	$3.0° \le 2\theta \le 45°$, $\theta-2\theta$		
scan width, deg	$\Delta\theta = 1.00 + 0.35(\tan\theta)$	$\Delta\theta = 0.80 + 0.35(\tan\theta)$	
octants collected	$+h,\pm k,\pm l$	$+h,\pm k,\pm l$	$+h,+k,+l$
reflections collected	7694	3848	1883
unique reflections	3848	3848	1339
reflections, $F_o^2 > 3\sigma(F_o^2)$	2945	2964	954
variables	325	325	109
R, %	4.22	4.81	4.36
R_w, %	5.40	6.26	5.80
R_{all}, %	6.01	6.17	6.74
GOF	1.694	1.962	2.096
largest Δ/σ in final LS cycle	0.01	0.01	0.00

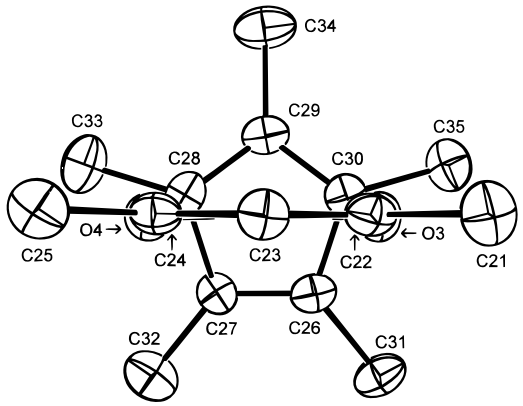

Figure 2. ORTEP diagram for one molecule of $(Me_5C_5)Ni(acac)$; the projection is along the only (noncrystallographic) symmetry element present, the plane of symmetry running through C23, C29, C34, and Co2 (obscured by C23).

The nickel compound is less well-behaved magnetically (Figure 3b). In the solid state, the plot of $(\chi_M)^{-1}$ vs *T* is nonlinear. Below *ca*. 150 K χ_M is less than zero, indicating a diamagnetic ground state (this is why Figure 3b shows χ_M vs *T*, not $(\chi_M)^{-1}$ vs *T*), but above this temperature χ_M becomes positive and increases with increasing temperature, indicating that the extent of paramagnetism increases with temperature. In solution, the magnetic moment is 1.3 μ_B at 303 K in C_6D_6. The nickel compound does not yield an EPR spectrum at room temperature or at 2 K, but in contrast to the cobalt compound, it does yield a ^{1}H NMR spectrum at 299 K in PhMe-d_8 that consists of three resonances at δ 63.4 ($\nu_{1/2}$ = 30 Hz), −2.32 ($\nu_{1/2}$ = 3 Hz), and −10.0 ($\nu_{1/2}$ = 5 Hz) due to Me_5C_5, CH, and COMe protons, respectively. The spectrum is temperature dependent as shown by the plots of δ (chemical shift) for each resonance relative to the inverse of the absolute temperature in Figure 4.[7] These plots also show nonlinear behavior with the chemical shifts moving to the diamagnetic region of the spectrum as temperature decreases. Consistent with the shift toward diamagnetism, the Me_5C_5 resonances sharpen on cooling so that by 193 K, $\nu_{1/2}$ is 10 Hz. The plots in Figure 4 also show that nearly identical traces are observed in toluene or tetrahydrofuran and that the methyl groups on the Me_5C_5 ring and the acetylacetonate ligand are chemically equivalent at all temperatures. The nonlinear behavior is consistent with the existence of a temperature dependent process or an equilibrium in solution, but this process is not a slowing of some fluxional process since the line shapes are invariant with temperature. The molecule is either highly symmetric or nonrigid throughout the temperature range; $Me_5C_5Ni(acac)$ is an 18-electron molecule that is paramagnetic at room temperature.

Table 4. Summary of Important Structural Parameters in "Ene−Allyl" Systems

compound	$d(M-C_a)^a$	$d(M-C_b)^a$	$d(M-C_c)^a$	Δ^b	ω^c
$(C_5Me_5)Ni(acac)$	2.133 (3)	2.068 (3)	2.192 (3)	0.124	9.3
$(C_5Me_5)Co(acac)$	2.105 (3)	2.056 (2)	2.089 (2)	0.033	4.2
$(C_5Me_5)Ni(Br)(PEt_3)$	2.159 (7)	2.098 (4)	2.154 (5)	0.056	5.2
$(C_5Me_5)Co(Cl)(PEt_3)$	2.119 (9)	2.058 (6)	2.075 (6)	0.017	3.2
$(C_5Me_5)Co(CO)_2$[10b]	2.102 (4)	2.067 (3)	2.103 (3)	0.036	
$[(C_5H_5)Ni(C_3H_4)]_2$[10a]	2.167 (4)	2.090 (3)	2.095 (3)	0.005	3.4

[a] Averaged values in Å. [b] $\Delta = |d(M-C_b) - d(M-C_c)|$. [c] Angle in degrees (value not reported for $(C_5Me_5)Co(CO)_2$[10b]). ω is the fold angle of the Cp ring due to selective population of the 5a′ orbital, *viz.*:

Coordination Complexes with PR_3. Synthesis and Solid State Properties. The cobalt compound does not yield an isolable coordination complex with PMe_3. Addition of PEt_3 to

(7) (a) LaMar, G. N.; Horrocks, W. D.; Holm, R. H. *NMR of Paramagnetic Molecules*; Academic Press: New York, 1973; Chapter 7. (b) Jahn, W.; Yünlü, K.; Oroschin, W.; Amberger, H. D.; Fischer, R. D. *Inorg. Chim. Acta* **1984**, *95*, 85. This paper presents an excellent description of δ vs T^{-1} plots.

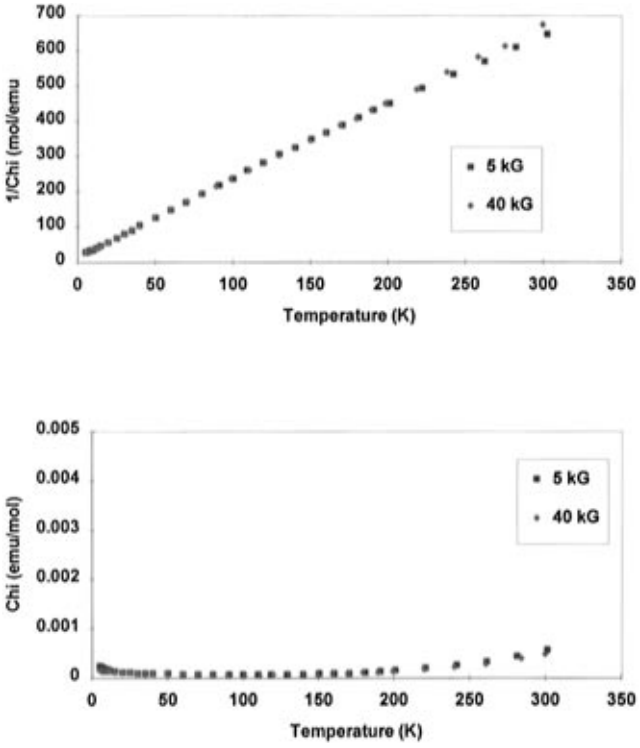

Figure 3. (a) Top: plot of $1/\chi_M$ vs T for $(Me_5C_5)Co(acac)$. (b) Bottom: plot of χ_M vs T for $(Me_5C_5)Ni(acac)$.

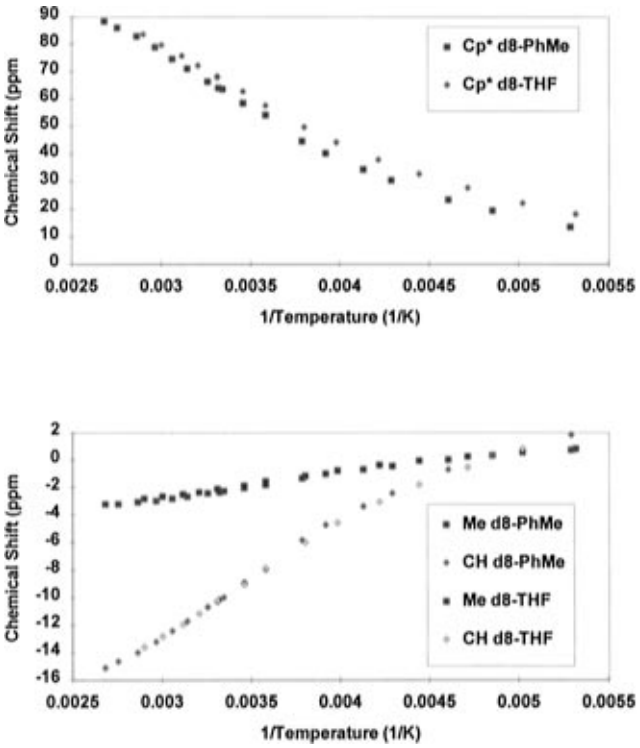

Figure 4. Plots of δ vs T^{-1} for ^1H NMR resonances of $(Me_5C_5)Ni(acac)$. (a) Top: Me_5C_5 resonances. (b) Bottom: acac resonances.

red $Me_5C_5Co(acac)$ yields an orange solution in pentane; only red $Me_5C_5Co(acac)$ is isolated upon crystallization. Since $Me_5C_5Co(acac)$ is ^1H NMR silent, we cannot use ^1H NMR spectroscopy to study this hypothetical equilibrium. In contrast, the nickel complex gives isolable complexes with either PMe_3 or PEt_3. An ORTEP diagram of $Me_5C_5Ni(acac)(PMe_3)$ is shown in Figure 5, along with some bond distances and angles. Two principal changes occur in the solid state when $Me_5C_5Ni(acac)$ bonds to PMe_3. All of the bond distances lengthen; the Ni−O

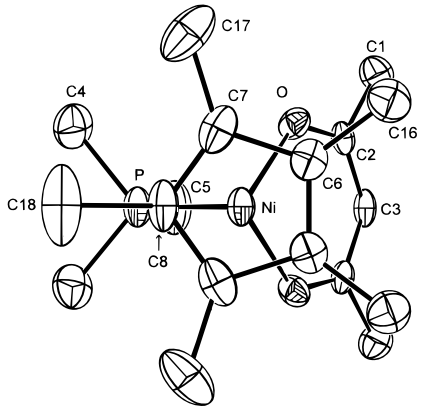

Figure 5. ORTEP diagram for $(Me_5C_5)Ni(acac)(PMe_3)$, 50% probability ellipsoids, projection along the crystallographically-imposed plane of symmetry. Ni−O = 2.035 (8) Å, Ni−P = 2.337 (2) Å, Ni−C (av) = 2.235 (4) Å, Ni−(Me_5C_5)centroid = 1.88 Å, O−Ni−O = 91.0 (2)°, O−Ni−P = 91.0(1)°, O−Ni−(Me_5C_5)centroid = 122°, P−Ni−(Me_5C_5)centroid = 130°.

and the Ni−C(av) lengthen by 0.16 and 0.13 Å, respectively, as expected since the coordination number of nickel increased by one unit. More importantly, the spread in Ni−C distances is small, 2.226 (5) to 2.249 (5) Å, and the C−C distances in the Me_5C_5 ring are equal within 4σ, ranging from 1.395 (11) to 1.437 (7) Å. Thus, the Me_5C_5 ring distortion that is observed in the base-free compound is largely absent in the PMe_3 compound. Further, the magnetic behavior shows the PMe_3 complex is paramagnetic in the solid state. A plot of $(\chi_M)^{-1}$ vs T is linear from 5 to 300 K, and μ_{eff} is 2.52 μ_B.

Solution Properties. In contrast to the cobalt case, the nickel compounds can be studied in solution by ^1H NMR spectroscopy. In solution, the PMe_3 adduct is paramagnetic, but all of the resonances are observed from *ca.* −20 °C to high temperature. A plot of δ vs T^{-1} is essentially linear throughout the high-temperature regime. Addition of PMe_3 does not shift the resonances at 30 °C, and a resonance is observed for free PMe_3 at δ 1.11. Thus, free and coordinated PMe_3 do not exchange on the NMR time scale, and no temperature dependent processes are occurring in solution over the temperature range studied, *i.e.*, $Me_5C_5Ni(acac)(PMe_3)$ is behaving as a simple paramagnet.

In contrast, the PEt_3 complex behaves differently. The chemical shifts of all of the resonances are nonlinear in temperature from *ca.* 0 to 100 °C. A plot of the chemical shifts of the resonances as a function of T^{-1} is shown in Figure 6 in absence of added PEt_3 and in the presence of added PEt_3. The resonances due to the CH_2 and CH_3 protons of the phosphine are averaged resonances over the temperature range and this allows them to be assigned with certainty. Further, the resonances shown in Figure 6 follow the same family of curves with or without added phosphine. The behavior of the resonances is consistent with a temperature dependent process occurring, and the nonlinear behavior is the result of the weighted average of the chemical shifts of all of the species present in solution. Since the chemical shifts depend upon the population of the individual species and their unique chemical shifts, which in turn depend upon temperature, the averaged chemical shifts are also temperature dependent. This temperature dependence is most likely the result of a rapid (on the NMR time scale) dissociative equilibrium between free and coordinated phosphine. Since PEt_3 is larger and more basic than PMe_3, the dissociative exchange is most reasonably ascribed to steric rather than electronic effects.[8]

(8) Tolman, C. A. *Chem. Rev.* **1977**, *77*, 313.

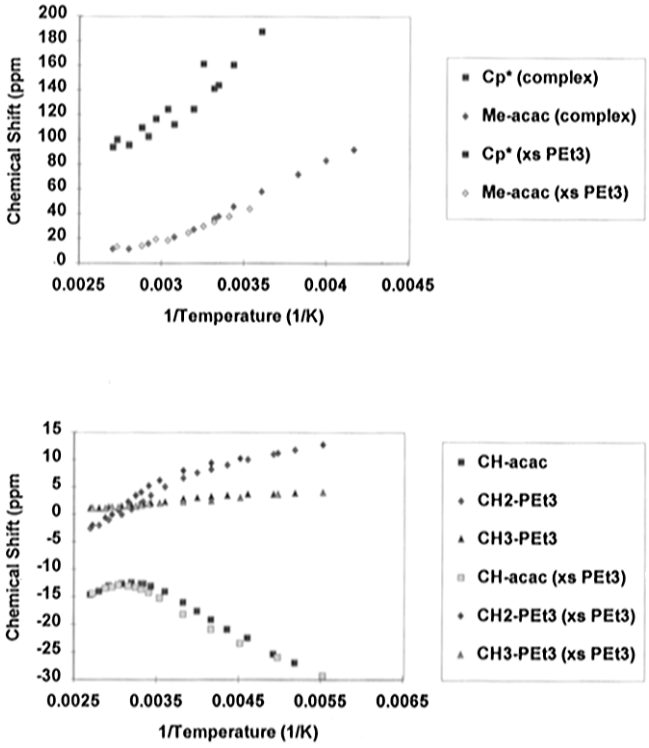

Figure 6. Plots of δ vs T^{-1} for ^{1}H NMR resonances of $(Me_5C_5)Ni(acac)(PEt_3)$. (a) Top: Me_5C_5 and Me resonance of acac. (b) Bottom: methyne resonance of acac and ethyl resonances of PEt_3.

Discussion

The types of distortions of the Me_5C_5 rings found in $Me_5C_5M(acac)$, M = Co, Ni, were discussed as early as 1963.[9] Distortions of the planar C_5R_5 group are to be expected in molecules of low molecular symmetry since the degeneracy in the doubly-degenerate e orbitals will be broken when the molecule has C_2 or lower rotational symmetry. The first example of such a distortion in the solid state was $[CpNi(C_3H_4)]_2$,[10a] and later $Me_5C_5Co(CO)_2$ was shown to have a similar distortion of the Me_5C_5 ring.[10b] It is noteworthy that Kettle is quoted in ref 9a as suggesting that the Cp ring in $CpCo(CO)_2$ should be distorted because the low molecular symmetry removes the degeneracy of the e^+ and e^- orbitals; a distortion that was found in $Me_5C_5Co(CO)_2$. Dahl's masterful discussion of the ring distortions found in $Me_5C_5Co(CO)_2$ has a strong influence on the discussion that follows. Indeed, $Me_5C_5Ni(acac)$ and $Me_5C_5Co(CO)_2$ are isoelectronic, both molecules are 18-electron compounds with d^8-metal centers, and both have idealized C_s symmetry in the solid state, which requires, in absence of crystallographic disorder, that the Me_5C_5 rings are noncylindrical. The only difference between these two molecules is that CO is a good π-acceptor ligand, while the acetylacetonate ligand is, at best, a poor π-donor ligand, and for simplicity will be viewed as a bidentate σ-donor ligand.

The symmetry orbital diagram for $Me_5C_5Ni(acac)$ is similar to that of $CpCo(CO)_2$ that is shown in Albright, Burdett, and Whangbo.[11a,c] The acac compounds have C_s symmetry, with the plane of symmetry bisecting the Me_5C_5 ring and M(acac) fragment, as can be seen in Figure 7. In C_s symmetry all of the symmetry orbitals transform as a′ or a″, *i.e.*, they are symmetric or antisymmetric relative to the molecular plane of symmetry, which was chosen, in this case, to lie in the *xz* plane

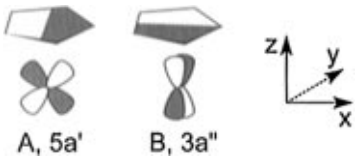

Figure 7. Representation of the HOMO (A) and LUMO (B) in 17- and 18-electron molecules of the type $CpML_2$ with C_s symmetry. The two ligands (or oxygen atoms of the bidentate acac ligand) lie above and below the plane of the paper along the *y* axis.

as shown in Figure 7. The discussion will center around the character of the HOMO and LUMO, since these two orbitals are chiefly responsible for the distortions of the Me_5C_5 ring. The HOMO of $Me_5C_5Ni(acac)$ is 5a′ and is shown as A in Figure 7. The LUMO is 3a″ and labeled B. In A, the metal orbital is of *xz* parentage; it is metal−ring antibonding and contains two electrons in $Me_5C_5Ni(acac)$ and one electron in $Me_5C_5Co(acac)$. In B, the metal orbital is of *yz* parentage, and it is also metal−ring antibonding but is empty. The noncylindrical metal−ring bonding can be understood since population of A results in puckering of the Me_5C_5 ring about the *y* axis (see Table 4). In addition, the selective population of A produces a lengthening of two C−C bonds and contracting of a third C−C bond, the one bisected by the mirror plane of symmetry, resulting in the ene−allyl distortion of the Me_5C_5 ring (see Table 2). Since $Me_5C_5Co(acac)$ contains one less electron in the HOMO, the antibonding interactions should be felt less strongly and the distortions accordingly less dramatic. This is what is observed, as shown in Table 4. So far, the simple symmetry model is sufficient to rationalize the solid state structures of these two compounds. How well does it fit the experimental data on the electronic structure?

The single electron in the cobalt compound resides in an orbital of a′ symmetry, and the ^{2}A ground state will yield an isotropic EPR spectrum at room temperature with an averaged *g* value near that of the free electron value of 2.0023. The observed average *g* value of 2.099 is greater than the free electron value, which means that the orbital contribution is not completely quenched. The orbital contribution is also the reason why the observed magnetic moment is greater than the spin-only moment of 1.73 μ_B. The symmetry orbitals developed above from simple theory show that the 5a′ and 3a″ orbitals are derived from metal orbitals of d_{xz} and d_{yz} parentage, respectively, and both have one unit of orbital angular momentum ($m_L = \pm 1$), so spin−orbit coupling can occur. The linear $(\chi_M)^{-1}$ vs *T* plot indicates that the energy difference (HOMO−LUMO gap) between the 5a′ and 3a″ orbitals (A and B) is either large, with B not populated, or rather small, so that both A and B are populated, but they have similar spin−orbit coupling values, so that the magnetic susceptibility is largely unaffected by changing temperature. The latter explanation seems more likely, for reasons which will be discussed shortly.

The inability to observe an EPR spectrum at room temperature or at temperatures approaching 4 K for $Me_5C_5Ni(acac)$ implies either that the electrons are coupled to give a diamagnetic compound throughout the temperature regime studied or that the compound is paramagnetic with one electron in each of two

(9) (a) Dahl, L. F.; Wei, C. H. *Inorg. Chem.* **1963**, *2*, 713. (b) Bennett, M. A.; Churchill, M. R.; Gerloch, M.; Mason, R. *Nature* **1964**, *201*, 1318.
(10) (a) Smith, A. E. *Inorg. Chem.* **1972**, *11*, 165. (b) Byers, L. R.; Dahl, L. F. *Inorg. Chem.* **1980**, *19*, 277.
(11) (a) Albright, T. A.; Burdett, J. K.; Whangbo, M. H. *Orbital Interactions in Chemistry*; Wiley: New York, 1985; p 370. (b) Albright, T. A.; Burdett, J. K.; Whangbo, M. H. *Orbital Interactions in Chemistry*; Wiley: New York, 1985; p 385. (c) The photoelectron spectroscopic studies are described in the following: Dudeney, N.; Kirchner, O. N.; Green, J. C.; Maitlis, P. M. *J. Chem. Soc., Dalton Trans.* **1984**, 1877. Lichtenberger, D. L.; Calabro, D. C.; Kellogg, G. E. *Organometallics* **1984**, *3*, 1623.
(12) Figgis, B. N. *Introduction to Ligand Fields*; Wiley: New York; 1966.

Table 5. Fittted Parameters for (Me_5C_5)Ni(acac) VT ^{1}H NMR Data

solvent	chemical shifts (ppm)			$\Delta H^{\circ a}$ (kcal/mol)	$\Delta S^{\circ a}$ (cal/(mol K))	$\Delta G^{\circ b}$ (kcal/mol)
	C_5Me_5	Me−acac	CH−acac			
toluene-d_8	5.62	1.29	3.87	2.72	7.56	0.47
tetrahydrofuran-d_8	9.72	1.32	3.34	2.67	7.29	0.50
average	7.67	1.31	3.61	2.70	7.43	0.49

[a] Average of curve-fitting results for all three signals. [b] Calculated for $T = 298$ K.

near-degenerate orbitals. The magnetism and ^{1}H NMR data support the latter explanation for the nickel compound at temperatures above *ca*. 150 K, which implies that the HOMO−LUMO gap is small for the diamagnetic ground state. The plot of $(\chi_M)^{-1}$ as a function of temperature is nonlinear. At temperatures below 150 K the molecule is diamagnetic; as temperature increases, so does the population of the paramagnetic excited state. Using the simple symmetry model, the ground state is diamagnetic with both electrons in the 5a′ (A) orbital, and as temperature increases, the 3a″ (B) orbital gets populated. This means that the HOMO−LUMO gap is less than kT (*ca*. 200 cm^{-1} at 273 K), and that $Me_5C_5Ni(acac)$ is a spin equilibrium molecule.

The small HOMO−LUMO gap in $Me_5C_5M(acac)$ and the large HOMO−LUMO gap in $Me_5C_5Co(CO)_2$ can be rationalized on the basis of the difference between the π-acceptor and π-donor orbitals of CO and acac.[11] For simplicity, the effect of π-acceptance on the 5a′ (A) and 3a″ (B) orbitals will be considered, since this will be where the principal differences arise. B will be unaffected since it has only σ-bonding symmetry with respect to the acac or CO ligands, so π-acceptance by these ligands will neither stabilize nor destabilize it. A will be strongly stabilized by π-accepting ligands since the overlap between the π orbitals of the ligands and the metal d_{xz} orbital is good. This will remove some of the destabilizing Me_5C_5 ring to metal antibonding interaction, and this is the reason why $Me_5C_5Co(CO)_2$ is a diamagnetic compound at room temperature. When the strong π-acceptor CO ligands are replaced with the weakly π-donating acac ligand, the 5a′ is destabilized and its energy moves closer to 3a″, thus shrinking the HOMO−LUMO gap.[13]

The variable temperature ^{1}H NMR results for $Me_5C_5Ni(acac)$ also point toward a spin equilibrium in solution. As shown in Figure 4, a plot of δ vs T^{-1} shows that the chemical shift behavior of the resonances is nonlinear in inverse temperature, and the nonlinear behavior is nearly identical in toluene and tetrahydrofuran solution, two solvents whose dielectric constants are quite different. This implies that the nonlinear behavior is not due to intermolecular processes occurring in solution, such as coordination of solvent or a bidentate−monodentate interconversion. Further, a stereochemically rigid structure (due to the ene−allyl distortion) should have inequivalent methyl ring resonances in the ratio of 1:2:2, but this is not observed; only a single Me_5C_5 resonance is observed to −80 °C. Clearly, some presumably intramolecular fluxional process which is rapid on the NMR time scale over the observable temperature regime is responsible for the single Me_5C_5 resonance. We cannot know what this process is since there is no information present in the line shapes of the resonances.

If our model of $Me_5C_5Ni(acac)$ is correct, *viz*., there is a spin equilibrium between a diamagnetic ground state and a paramagnetic triplet excited state, then the ^{1}H NMR spectra should be modeled by using a simple Boltzmann distribution of spins. This theory has been developed and applied to spin equilibrium in octahedral Co(III) complexes, in which the following formula has been used to fit NMR data

$$\delta = \delta_{ls} + \frac{C}{T[1 + e^{(\Delta H^\circ - T\Delta S^\circ)/RT}]}$$

where δ is the observed chemical shift, δ_{ls} is the calculated shift for the diamagnetic species, ΔH° and ΔS° are the enthalpy and entropy, respectively, of the transition between low-spin and high-spin states, T is the absolute temperature, and C is a constant related to the molar susceptibility of the high-spin species.[14] The results of the fitting for (C_5Me_5)Ni(acac), where the equilibrium is between the diamagnetic ground state and the spin-triplet excited state, are shown in Table 5. All of the thermodynamic values agree well with each other, and the extrapolated diamagnetic shifts are reasonably close to those expected for diamagnetic compounds except for the C_5Me_5 signal. However, the error in this value is large, since the signal is several hundred hertz wide and shifts over nearly 90 ppm in the temperature range studied. The change in entropy is positive because the high-spin state has more vibrational and rotational degrees of freedom. The change in enthalpy is also positive because the metal radius is smaller for the low-spin state and the bonds are shorter and presumably stronger for the low-spin state since there are no electrons in the strongly metal−ligand antibonding 3a″ orbital. These two contrary effects are in competition in this example so that ΔH° favors the low-spin species at low temperatures, even though the pairing energy is necessarily endothermic, and the $T\Delta S^\circ$ term dominates at high temperatures, favoring the high-spin species. The values found yield a high-spin−low-spin equilibrium constant (K_{eq}) of 0.47 at 30 °C, where K_{eq} = [% high-spin]/[% low-spin].

The simple model used to rationalize the solid state distortions and solution behavior of $Me_5C_5M(acac)$ compounds is also able to rationalize the molecular and electronic structure of the phosphine coordination complexes. As before, for simplicity the symmetry orbitals for $CpMn(CO)_3$ in C_s symmetry will be the starting point for $Me_5C_5Ni(acac)(PMe_3)$, replacing three π-acceptor ligands with a bidentate weak π-donor ligand and a monodentate σ-donor.[11b] As shown in ref 11b, the 2e orbitals are stabilized by π-acceptors, so replacing the CO ligands with σ-donors destabilizes this pair of orbitals while stabilizing the 3e pair of orbitals. For $Me_5C_5Ni(acac)(PMe_3)$, the HOMO (the 3e orbital set) is half occupied by two electrons, but upon transforming to C_s symmetry from pseudo-C_{3v} symmetry, the orbitals are no longer degenerate and transform as a′ and a″. These orbitals are of metal d_{xz} and d_{yz} parentage, and they are similar to those symbolized as A and B in Figure 7, *viz*., they are metal−ring antibonding.

The solid state X-ray crystallographic results can be rationalized by this simple model. The spread in the Ni−C distances is smaller, 2.226 (5) to 2.249 (5) Å), than that found in the base-free compound, as is the spread in C−C distances; no ene−

(13) (a) Kläui, W.; Schmidt, K.; Bockmann, A.; Hofmann, P.; Schmidt, H.; Stauffert, P. *J. Organomet. Chem.* **1985**, *286*, 407. (b) Kläui, W.; Schmidt, K.; Bockmann, A.; Brauer, D. J.; Wilke, J.; Lueken, H.; Elsenhans, U. *Inorg. Chem.* **1986**, *25*, 4125. (c) Werner, H.; Ulrich, B.; Schubert, U.; Hofmann, P.; Zimmer-Gasser, B. *J. Organomet. Chem.* **1985**, *297*, 27.

(14) (a) Gütlich, P.; McGarvey, B. R.; Kläui, W. *Inorg. Chem.* **1980**, *19*, 3704. (b) Kläui, W.; Eberspach, W.; Gütlich, P. *Inorg. Chem.* **1987**, *26*, 3977.

allyl distortion is apparent in $Me_5C_5Ni(acac)(PMe_3)$. This is the expected result if the a″ and a′ orbitals are approximately equal in energy, and hence roughly equally populated, indicating that the metal−ring antibonding is essentially equal in both the d_{xz} and d_{yz} interactions. This is the case because the acac and PMe_3 ligands have generally similar electronic bonding properties in this complex, as compared to CO; that is, both acac and PMe_3 act as good σ-donors and poor or negligible π-donors. This deduction is supported by the solid state magnetic susceptibility and solution ^{1}H NMR spectroscopic results. The plot of $(\chi_M)^{-1}$ as a function of absolute temperatures is linear, indicating that over the temperature range observed, the orbital populations are not changing very much. Even at low temperature the trace is linear, implying that the separation of the two orbitals of 3e "parentage" is much less than kT. The solution behavior is also normal, since the plot of the chemical shift for all of the resonances is linear in T^{-1}, implying that no temperature dependent equilibria are operating in solution, unlike the PEt_3 complex. Thus, the 20-electron PMe_3 complex is electronically similar to the classic metallocenes Cp_2Ni and $(Me_5C_5)_2Ni$.[15]

It is unfortunate that the coordination complex of $Me_5C_5Co(acac)$ could not be isolated since the complex would have unequally populated a′ and a″ orbitals, and therefore an ene−allyl distortion of the Me_5C_5 ring, if our model is correct. The reason for our inability to isolate this complex is not obvious, but an orbital symmetry reason might be suggested. The HOMO of the base-free compound is 5a′, symbolized by A. The LUMO must be of the same symmetry and energy as the entering σ-donor. A symmetry orbital, symbolized by B, is available, but its energy is rather different from the σ-donor orbital in PMe_3, so the inability to isolate the complex might be traced to the poor orbital overlap and energy match in the adduct. In nickel the orbital energies are somewhat lower so better overlap can occur.

Other Systems. The postulate that the HOMO of isoelectronic $CpCo(CO)_2$ and $Me_5C_5Ni(acac)$ are identical allowed us to rationalize the ene−allyl distortion in the latter compound. The magnetic properties of these two compounds are very different as the carbonyl is low spin, whereas the Ni(acac) compound is a spin equilibrium molecule with a diamagnetic ground state. The origin of this difference lies in the effect on the HOMO of ligands that are π-acceptors relative to those that are π-donors.[13] This simple operational model can be tested by preparing compounds in which the bidentate acetylacetonate ligand is replaced by two monodentate ligands, such as halide or alkyl and a phosphine. We have prepared $Me_5C_5Ni(Br)(PEt_3)$ and $Me_5C_5Ni(CH_3)(PEt_3)$.[16,17] Both of these compounds are diamagnetic in solution and in the solid state, so no spin equilibrium is observed, presumably because the HOMO−LUMO gap is greater than kT. The crystal structure of the bromide shows an ene−allyl distortion, the extent of which is between that found for $CpCo(CO)_2$ and $Me_5C_5Ni(acac)$ (Table 4). Further, the extent of the solid state distortion is greater in nickel bromide than in $Me_5C_5Co(Cl)(PEt_3)$, *i.e.*, the metals with d^8 electronic configuration have Me_5C_5 ring distortions that are greater than those of otherwise closely related d^7 ones. Unfortunately, the solid state structure of $Me_5C_5Ni(CH_3)(PEt_3)$ suffers from disorder, and it is not sufficiently accurate to identify distortions. These results show that ligands play an important and, to a certain extent, predictable role in the molecular and electronic structures in 18-electron molecules of the type $Me_5C_5Ni(X)(Y)$.

The analogy that was developed to connect the symmetry orbitals of $CpCo(CO)_2$ and $CpMn(CO)_3$ with those of $Me_5C_5Ni(acac)$ and its PMe_3 complex can be developed further in terms of ligand substitution reactions. Exchange of CO with $CpCo(CO)_2$ proceeds by way of an associative pathway even though it is an 18-electron compound. It was proposed that the Cp ring slips in the transition state, opening a site for coordination.[18] The ground state of $CpCo(CO)_2$ is already distorted, with the ene−allyl distortion placing the Cp ring in a position intermediate to that of η^5 and η^3 coordination, so a ring slip should be a small reorganization of the molecular geometry. The structural features found for $Me_5C_5Ni(acac)$ and its PMe_3 complex seem to be reasonable structural models for the distortion of the Cp ring along the reaction coordinate of $CpCo(CO)_2 + {}^*CO \rightarrow CpCo({}^*CO)(CO)_2 \rightarrow CpCo({}^*CO)(CO) + CO$. The ground state distortions in $CpCo(CO)_2$ and $Me_5C_5Ni(acac)$ are similar. Addition of PMe_3 to the latter generates an isolable 20-electron complex that should mimic the transition state in the CO exchange reaction, *i.e.*, the Ni−C bonds are stretched, and the Cp ring has cylindrical symmetry. Although the spin state does change in the nickel example, the change in structural details in the base-free and PMe_3 complexes are useful transition state models.[19]

Using the language of coordination chemistry, the structure of $Me_5C_5Ni(acac)$ can be described as square-planar Ni(II) with a low-spin d^8 electron configuration in the ground state. The view presented in Figure 2 exemplifies this viewpoint, and the diamagnetic ground state follows naturally. Interconversion between square-planar, diamagnetic and tetrahedral, paramagnetic isomers has been extensively studied, and $Me_5C_5Ni(acac)$ has much in common with classical coordination complexes.[20] Extending the analogy further, the PMe_3 complex is an example of octahedral nickel(II) (the Me_5C_5 ligand occupying three facial sites since it is symmetrically bonded to nickel), and the high-spin state is not unexpected. In a further extension, replacing the bidentate acac ligand with a monodentate ligand gives the five-coordinate $Me_5C_5Ni(X)(PR_3)$ complexes, which are diamagnetic. In this context, it is instructive to recall that $Me_5C_5Fe(acac)(PMe_3)$ is said to be paramagnetic since the ^{1}H NMR resonances are broad and the chemical shifts are temperature dependent.[21a] Using coordination chemistry language, the complex is Fe(II) d^6 and expected to be low-spin in its octahedral crystal field. If phosphine dissociation is rapid, the five-coordinate base-free complex, which should be paramagnetic, could be the source of the paramagnetic behavior observed in the ^{1}H NMR spectrum.

The 18-electron cation, $Me_5C_5Fe(dppe)(Me_2CO)^+$, isoelectronic with $Me_5C_5Ni(acac)$ and $Me_5C_5Fe(acac)(PMe_3)$, is paramagnetic in the solid state from 77 to 300 K, $\mu = 2.9\ \mu_B$, and

(15) (a) Green, M. L. H. *Organometallic Compounds: The Transition Metals*; Methuen: London, **1968**; Vol. 2. (b) Grebenik, P.; Grinter, R.; Perutz, R. N. *Q. Rev., Chem. Soc.* **1988**, 453. (c) Robbins, J. L.; Edelstein, N. M.; Spencer, B.; Smart, J. C. *J. Am. Chem. Soc.* **1982**, *104*, 1882.

(16) A manuscript describing these and other data will be submitted shortly. Holland, P. L.; Smith, M. E.; Bergman, R. G.; Andersen, R. A. Manuscript in preparation.

(17) Werner, H.; Kraus, H.-J.; Schubert, U.; Ackermann, K.; Hoffmann, P. *J. Organomet. Chem.* **1983**, *250*, 517. The isoelectronic system η^5-CpPd(η^1-Cp)PR_3 is prepared and discussed using fragments based on symmetry orbitals in this reference.

(18) (a) Wojcicki, A.; Basolo, F. *J. Inorg. Nucl. Chem.* **1961**, *17*, 77. (b) Rerek, M. E.; Basolo, F. *Organometallics* **1983**, *2*, 372.

(19) (a) Hofmann, P. *Angew. Chem., Int. Ed. Engl.* **1977**, *16*, 536. (b) Hofmann, P.; Padmanabhan, M. *Organometallics* **1983**, *2*, 1273. (c) Dudeney, N.; Kirchner, O. N.; Green, J. C.; Maitlis, P. M. *J. Chem. Soc., Dalton Trans.* **1984**, 1877.

(20) (a) Holm, R. H. *J. Am. Chem. Soc.*, **1961**, *83*, 4683. (b) Succoni, L.; Paoletti, P.; Ciampolini, M. *J. Am. Chem. Soc.* **1963**, *85*, 411. (c) Holm, R. H.; O'Connor, M. J. *Prog. Inorg. Chem.* **1971**, *14*, 241.

(21) (a) Paciello, R. A.; Manriquez, J. M.; Bercaw, J. E. *Organometallics*, **1990**, *9*, 260. (b) Hamon, P.; Toupet, L.; Hamon, J.-P.; Lapinte, C. *J. Chem. Soc., Chem. Commun.*, **1994**, 931.

in acetone solution at room temperature.[21b] The paramagnetism can be understood by the same model used for $Me_5C_5Ni(acac)$, *viz.*, the HOMO−LUMO gap is decreased as a result of the σ-donor ligands. Dissociation of acetone, giving a 16-electron cation, cannot be excluded by the data presented, but two species are detected in the powder EPR spectrum at 77 K.

Experimental Section

All reactions and product manipulations were carried out under an atmosphere of dry nitrogen using standard Schlenk and drybox techniques. Infrared spectra were recorded on a Nicolet 5DX FTIR spectrometer as Nujol mulls between CsI or KBr plates. All ^1H, ^{13}C, and $^{31}P\{^1H\}$ nuclear magnetic resonance spectra were measured on a JEOL FX90Q FT NMR spectrometer operating at 89.6 (^1H) or 23.6 (^{13}C) MHz. Electron paramagnetic resonance spectra were recorded on an IBM ER-2090D-SRC spectrometer and were measured in methylcyclohexane (solution or glass) unless otherwise noted. Simulation of the EPR spectra was accomplished by comparison of experimental spectra with calculated spectra obtained from a second-order calculation program written by Dr. E. Gamp and run on a SUN MP630 computer server. EPR spectra with rhombic symmetry have three **g**-tensors, $\mathbf{g}_1$, $\mathbf{g}_2$, $\mathbf{g}_3$, and these labels were arbitrarily assigned so that $\mathbf{g}_1 < \mathbf{g}_2 < \mathbf{g}_3$. Absolute assignment of the **g**-tensors is impossible since the relative orientation of the crystallographic and magnetic axes in the glass is not known. Melting points were measured on a Thomas-Hoover melting point apparatus in sealed capillaries and are uncorrected. Solution magnetic moments were determined using the method described by Evans[22] using the aforementioned JEOL FX90Q FT NMR spectrometer. Solid state magnetic susceptibility measurements (SQUID) were obtained from either a S. H. E. Corporation Model 905 or a Quantum Designs MPMS HP-150 superconducting magnetometer. Samples were prepared and handled as previously described.[23] In all cases, the samples were purified by crystallization followed by sublimation, when possible. Susceptibility data were corrected for sample and container diamagnetism, and the data was treated as described previously.[23] Electron impact and fast-atom bombardment mass spectra were recorded by the mass spectrometry laboratory at the University of California, Berkeley. When molecular ions were observed, the isotopic cluster was reported as follows: ion amu (observed intensity, calculated intensity). Elemental analyses were performed by the analytical laboratories at the University of California, Berkeley.

$(C_5Me_5)Co(acac)$. A solution of bis(pentamethylcyclopentadienyl)-magnesium[6] (1.15 g, 3.90 mmol) in tetrahydrofuran (75 mL) was added to a slurry of bis(2,4-pentanedionato)cobalt(II)[24] (2.01 g, 7.82 mmol) in tetrahydrofuran (50 mL). Upon being mixed, the solution immediately changed color from pink to deep red. After the solution was stirred at room temperature for 1 h, the volatile materials were completely removed under reduced pressure, and the residue was extracted with diethyl ether (125 mL). The deep red solution was filtered, and the filtrate was concentrated to *ca*. 40 mL. Cooling to −80 °C afforded deep red plates. Concentration of the mother liquor provided an additional crop of crystals for a total yield of 1.86 g (6.34 mmol, 81.1% yield). Sublimation at 60 °C under dynamic vacuum (oil diffusion pump) is necessary to separate $(C_5Me_5)Co(acac)$ from a minor volatile impurity. Mp: 112−113 °C. IR: 2743 (w), 2723 (w), 2457 (w), 1958 (w), 1530 (vs), 1383 (s), 1365 (s), 1281 (s), 1193 (m), 1161 (m), 1069 (m), 1025 (s), 935 (m), 798 (s), 780 (s), 686 (w), 660 (m), 634 (m), 626 (m), 590 (w), 470 (s), 420 (m), 398 (m), 352 (w). No resonances were observed in the ^1H NMR spectrum in C_6D_6 at room temperature. EIMS: 293 (100, 100), 294 (17, 19), 295 (2, 2). Magnetic susceptibility (5−300 K): 5 kG, $\mu_{eff} = 1.94\ \mu_B$, $\theta = -8.69$ K; 40 kG, $\mu_{eff} = 1.91\ \mu_B$, $\theta = -6.53$ K. Solution magnetic moment (303 K, C_6D_6, 90 MHz): 1.86 μ_B. EPR: 298 K, $g_0 = 2.099$, $A_0 = 45.17$ G; 2 K, $g_1 = 1.970$, $A_1 = 43.11$ G, $g_2 = 2.091$, A_2 was not observed due to line width, $g_3 = 2.241$, $A_3 = 105.47$ G.

$(C_5Me_5)Ni(acac)$. A solution of bis(pentamethylcyclopentadienyl)-magnesium[6] (1.76 g, 5.97 mmol) in tetrahydrofuran (70 mL) was added to a solution of bis(2,4-pentanedionato)nickel(II)[24] (3.01 g, 11.7 mmol) in tetrahydrofuran (70 mL). Upon being mixed, the solution immediately changed color from bright green to deep red. After the solution was stirred at room temperature for 1 h, the volatile materials were completely removed under reduced pressure, and the residue was extracted with diethyl ether (150 mL). The deep red solution was filtered, and the filtrate was concentrated to *ca*. 60 mL. Cooling to −80 °C afforded deep red plates. Concentration of the mother liquor provided an additional crop of crystals for a total yield of 2.89 g (9.86 mmol, 84.3% yield). Mp: 98−99 °C. IR: 2735 (w), 2721 (w), 2453 (w), 1956 (w), 1550 (vs), 1390 (vs), 1376 (s), 1262 (s), 1196 (m), 1154 (m), 1066 (w), 1022 (s), 933 (s), 791 (s), 775 (s), 687 (w), 659 (m), 627 (m), 619 (m), 587 (w), 464 (s), 420 (m), 386 (m), 356 (w). ^1H NMR (C_7D_8, 299 K, 90 MHz): δ 63.40 (15H, C_5Me_5, $\nu_{1/2} = 30$ Hz), −2.32 (6H, acac−CH_3, $\nu_{1/2} = 3$ Hz), −10.04 (1H, acac−CH, $\nu_{1/2} = 5$ Hz). EIMS: 292 (100, 100), 293 (17, 18), 294 (40, 39), 295 (8, 8), 296 (6, 6). Solution magnetic moment (303 K, C_6D_6, 90 MHz): 1.32 μ_B. Magnetic susceptibility measurements (5−300 K) have $\chi_M < 0$ below ∼140 K, and $\chi_M > 0$ above this temperature.

$(C_5Me_5)Ni(acac)PMe_3$. To a solution of sublimed $(C_5Me_5)Ni(acac)$ (0.30 g, 1.0 mmol) in pentane (40 mL) was added 0.11 mL of trimethylphosphine (1.1 mmol). Upon being mixed, the solution immediately changed color from red to red-orange. After being stirred at room temperature for 15 min, the solution was concentrated to *ca*. 20 mL. Cooling to −80 °C afforded red-orange plates. Concentration of the mother liquor provided an additional crop of crystals for a total yield of 0.35 g (0.95 mmol, 93% yield). Mp: 75−77 °C. IR: 3078 (w), 2742 (w), 2718 (w), 1594 (vs), 1514 (s), 1400 (vs), 1320 (sh), 1304 (m), 1284 (m), 1254 (m), 1194 (m), 1014 (m), 949 (s), 919 (m), 839 (m), 797 (w), 791 (w), 755 (m), 733 (m), 671 (w), 651 (w), 629 (w), 619 (w), 557 (m), 465 (w), 409 (m). ^1H NMR (C_7D_8, 297 K, 90 MHz): δ 202 (15H, C_5Me_5, $\nu_{1/2} = 300$ Hz), 69.6 (6H, acac−CH_3, $\nu_{1/2} = 145$ Hz), 5.80 (9H, PCH_3, $\nu_{1/2} = 20$ Hz), −14.74 (1H, acac−CH, $\nu_{1/2} = 35$ Hz). Anal. Calcd for $C_{18}H_{31}NiO_2P$: C, 58.6; H, 8.46. Found: C, 58.3; H, 7.89.

$(C_5Me_5)Ni(acac)PEt_3$. To a solution of sublimed $(C_5Me_5)Ni(acac)$ (0.34 g, 1.2 mmol) in pentane (50 mL) was added 0.17 mL of triethylphosphine (1.2 mmol). Upon being mixed, the solution immediately changed color from red to red-orange. After being stirred at room temperature for 15 min, the solution was concentrated to *ca*. 25 mL. Cooling to −80 °C afforded very thin red-orange plates. Concentration of the mother liquor provided an additional crop of crystals for a total yield of 0.38 g (0.92 mmol, 80% yield). Mp: 79−81 °C. IR: 3072 (m), 2741 (w), 2725 (w), 1595 (s), 1509 (s), 1402 (vs), 1380 (m), 1370 (m), 1331 (sh), 1254 (s), 1190 (m), 1039 (s), 1013 (m), 919 (m), 763 (s), 719 (m), 701 (w), 667 (w), 652 (w), 626 (w), 554 (m), 462 (w), 406 (m). ^1H NMR (C_7D_8, 301 K, 90 MHz): δ 141.3 (15H, C_5Me_5, $\nu_{1/2} = 325$ Hz), 36.1 (6H, acac−CH_3, $\nu_{1/2} = 145$ Hz), 2.22 (6H, PCH_2CH$_3$, $\nu_{1/2} = 15$ Hz), 1.92 (9H, PCH$_2$CH_3, $\nu_{1/2} = 20$ Hz), −12.6 (1H, acac−CH, $\nu_{1/2} = 30$ Hz). Anal. Calcd for $C_{21}H_{37}NiO_2P$: C, 61.3; H, 9.07. Found: C, 61.4; H, 9.31.

Crystallographic Studies. Specific information pertaining to an individual crystal structure will be listed after the general procedure, under the name of the compound.

General Procedure. A crystal of appropriate dimensions was isolated and placed in Paratone N oil.[25] The crystal was mounted on the end of a cut quartz capillary tube and placed under a flow of cold nitrogen on an Enraf-Nonius CAD4 diffractometer.[26] The solidified oil held the crystal in place and protected it from the atmosphere. The temperature was stabilized with an automated flow apparatus. After the crystal was centered in the X-ray beam, a set of accurate cell dimensions and an orientation matrix were determined by a least squares

(22) (a) Evans, D. F. *J. Chem. Soc.* **1959**, 2003. (b) Baker, M. V.; Field, L. D.; Hambley, T. W. *Inorg. Chem.* **1988**, *27*, 2872.

(23) Berg, D. J.; Burns, C. J.; Andersen, R. A.; Zalkin, A. *Organometallics* **1989**, *8*, 1865.

(24) Charles, R. G.; Pawlikowski, M. A. *J. Phys. Chem.* **1958**, *62*, 440.

(25) Paratone N oil is a viscous commercial oil available from Exxon Chemical Co., Houston, TX. The oil was degassed prior to use.

(26) Instrumentation at the University of California Chemistry Department X-ray Crystallographic Facility (CHEXRAY) consists of two Enraf-Nonius CAD-4 diffractometers controlled by a DEC Microvax II and equipped with departmentally constructed low-temperature systems. Both use Enraf-Nonius software as described in the *CAD-4 Operations Manual*, *Version 5.0*; Enraf-Nonius: Delft, The Netherlands, 1977; updated 1989.

fit to the setting angles of the unresolved Mo Kα components of 24 symmetry-related reflections. Details of the crystal dimensions, unit cell, collection parameters and temperatures, and structure refinement are listed in Table 3.

A set of three standard reflections was chosen to monitor intensity and crystal orientation. The intensity was checked after every hour of X-ray exposure time. The crystal orientation was checked after every 200 reflections and was reoriented if any of the standard reflections were offset from their predicted position by more than 0.1°.

The raw data were converted to structure factor amplitudes and their esd's by correction for scan speed, background, and Lorentz-polarization effects.[27,28,29] An empirical absorption correction based on averaged azimuthal ψ-scans for three reflections with $\chi > 80°$[30] was initially attempted for each structure. If the ψ-scans did not correlate well (indicating that the scans would not accurately represent the crystal morphology), then the initial refinements were performed on uncorrected data and an empirical absorption correction was applied to the resulting solution using a Fourier series determined by minimizing the sum of the squares of the residuals, using the correction program provided with the MoLEN structure analysis package (DIFABS).[28b]

The coordinates of the heavy atoms (cobalt, nickel, phosphorus) were determined by either Patterson methods or direct methods (SHELXS).[31] The locations of all non-hydrogen atoms were determined through the use of standard Fourier techniques and refined by least squares methods. All non-hydrogen atoms were refined anisotropically. A difference Fourier map revealed the positions of all hydrogen atoms unless otherwise noted. These atoms were placed in calculated positions and included in the structure factor calculations, but not refined. All hydrogen atoms were given isotropic thermal parameters 1.3 times the *B*(iso) of the atom to which they were bonded.

Final refinement of the variables using the data for which $F_o^2 > 3\sigma(F_o^2)$ gave the residuals R and R_w (see Table 3). The R value based on all unique data (R_{all}) and the goodness-of-fit parameter are also reported in Table 3. The least squares program minimized the expression, $\sum w(|F_o| - |F_c|)^2$, where w is the weight of a given observation. A value of 0.05 for the *p*-factor was used to reduce the weight of intense reflections in the refinements unless otherwise noted.[32] The analytical forms of the scattering factor tables for the neutral atoms[33] were used, and all non-hydrogen scattering factors were corrected for both real and imaginary components of anomalous dispersion.[34] The data were evaluated through the residuals over ranges of sin θ/λ, $|F_o|$, parity, and individual indices. Any unusual features or trends observed are listed below. The highest and lowest peaks in the final difference Fourier map in all cases were associated with the metal atoms.

(C_5Me_5)Co(acac). Clear red prisms of the complex were grown by sublimation at 60 °C at 10^{-4} Torr. The dimensions and volume of the unit cell suggested triclinic symmetry for 4 molecules in the unit cell. The set of three standard reflections used was (2, 5, −6; −6, −7, 8; 2, −1, −8) (after transformation, see below). Intensity checks showed no appreciable decay over the course of the data collection; the crystal orientation matrix did not reorient during the data collection. The DIFABS[28b] program was used for the empirical absorption correction; maximum correction was 17%.

Analysis of the data revealed the following systematic absences: *h*,*k*,*l*, $h + k$ odd, consistent with a nonprimitive doubled cell with C-centering. Upon transformation to a primitive cell, the 3848 remaining reflections showed no systematic absences, consistent with the space group $P\bar{1}$ (No. 2). The coordinates of the cobalt atoms were determined by Patterson methods. The highest and lowest peaks in the final difference Fourier map had electron densities of 0.53 and −0.12 e/Å^3, respectively.

(C_5Me_5)Ni(acac). Clear red plates of the complex were grown from a pentane solution at −80 °C. The dimensions and volume of the unit cell suggested triclinic symmetry with two molecules in the unit cell. The set of three standard reflections used was (3,5,8; −4,−4,2; 0,3,−7). Intensity checks showed no appreciable decay over the course of the data collection; the crystal orientation matrix was reoriented one time during the data collection. ψ-Scans were used for the empirical absorption correction; examination of the azimuthal scans showed a variation of $I_{min}/I_{max} = 0.84$ for the average relative intensity curve.

Evaluation of the data through the residuals over ranges of sin θ/λ, $|F_o|$, parity, and individual indices revealed systematic groups of two to four "clipped" peaks scattered throughout the data set. A total of 114 data were rejected as "bad" before the structure refined properly. The problem resulted from a peculiarity in crystal mounting that caused misalignment of reflections with very high χ. The intensities measured were erroneously low because of clipping of the peaks, as judged by inspection of the peak profiles. The crystal had already been disposed of when the trend was identified, precluding remounting of the crystal and recollection of the data set. The data set did not exhibit systematic absences, consistent with the space group $P\bar{1}$ (No. 2). The coordinates of the nickel atoms were determined by direct methods (SHELXS).[31]

(27) All calculations were performed on a DEC Microvax II or a DEC Microvax 4000 using locally modified Nonius-SDP software operating under the Micro-VMS operating system.

(28) (a) Frenz, B. A. *Structure Determination Package Users Guide*; Texas A & M University and Enraf-Nonius: College Station, TX, and The Netherlands, 1985. (b) Fair, C. K. *MoLEN Molecular Structure Solution Procedures*; Enraf-Nonius, Delft Instruments, X-ray Diffraction B. V.: The Netherlands, 1990.

(29) The data reduction formulas are

$$F_o^2 = \frac{\omega}{L_p}(C - 2B)$$

$$F_o = (F_o^2)^{1/2}$$

$$\sigma_o(F_o^2) = \frac{\omega}{L_p}(C + 4B)^{1/2}$$

$$\sigma_o(F) = [F_o^2 + \sigma_o(F_o^2)]^{1/2} - F_o$$

where C is the total count in the scan, B is the sum of the two background counts, ω is the scan speed used in deg/min, and

$$\frac{1}{L_p} = \frac{\sin 2\theta\,(1 + \cos^2 2\theta_m)}{1 + \cos^2 2\theta_m - \sin^2 2\theta}$$

is the correction for Lorentz and polarization effects for a reflection with scattering angle 2θ and radiation monochromatized with a 50% perfect single-crystal monochromator with scattering angle $2\theta_m$.

(30) Reflection used for azimuthal scans were located near $\chi = 90°$, and the intensities were measured at 10° increments of rotation of the crystal about the diffraction vector.

(31) SHELXS-86 is a public domain direct methods solution algorithm written by G. M. Sheldrick; see: *Crystallographic Computing 3*; Sheldrick, G. M., Krüger, C., Goddard, R., Eds.; Oxford University Press: Oxford, 1985; pp 175−189.

(32)

$$R = \frac{\sum ||F_o| - |F_c||}{\sum |F_o|}$$

$$R_w \sqrt{\frac{\sum w(|F_o| - |F_c|)^2}{\sum w F_o^2}}$$

$$\mathrm{GOF} = \sqrt{\frac{\sum w(|F_o| - |F_c|)^2}{(n_o - n_v)}}$$

where n_o is the number of observations, n_v is the number of variable parameters, and the weights, w, are given by

$$w = \frac{1}{\sigma^2(F_o)}$$

$$\sigma(F_o^2) = \sqrt{\sigma_o^2(F_o^2) + (pF^2)^2}$$

where $\sigma^2(F_o)$ was calculated as above from $\sigma(F_o^2)$ and where p is the factor used to lower the weight of intense reflections.

(33) Cromer, D. T.; Waber, J. T. *International Tables for X-ray Crystallography*; The Kynoch Press: Birmingham, England, 1974; Vol. IV, Table 2.2B.

(34) Cromer, D. T. *International Tables for X-ray Crystallography*; The Kynoch Press: Birmingham, England, 1974; Vol. IV, Table 2.3.1.

The highest and lowest peaks in the final difference Fourier map had electron densities of 0.89 and −0.17 e/Å^3, respectively.

(C_5Me_5)Ni(acac)PMe_3. Red-orange plates of the complex were grown from a pentane solution at −80 °C. The dimensions and volume of the unit cell suggested orthorhombic symmetry with four molecules in the unit cell. The set of three standard reflections used was (6,2,−1; 1,7,4; 1,−1,8). Intensity checks showed an abrupt fading near the middle of the data collection (from reflections 4,0,0 to 6,6,2) due to loss of X-ray flux from the tube. After correction of the instrumental problem, intensity checks indicated that the crystal had not degraded. The region from 4,0,0 to 6,6,2 was duplicated by recollection at the end of the data set and the initial values of these reflections were discarded, yielding a final total of 1339 reflections. The crystal orientation matrix was reoriented two times during the data collection. The DIFABS[28b] program was used for the empirical absorption correction; maximum correction was 15%.

Analysis of the data revealed the following systematic absences: *h*,*k*,0, h odd; 0,*k*,*l*, *k* + l odd, consistent with the space group *Pnma* (No. 62). The coordinates of the nickel and phosphorus atoms were determined by Patterson methods. A difference Fourier map revealed the positions of all hydrogen atoms not lying on the mirror plane. The hydrogen atoms lying on the mirror plane were placed at their predicted positions, assuming a tetrahedral disposition of the methyl hydrogens and a C−H bond length of 0.95 Å. A value of 0.04 for the *p*-factor was used to reduce the weight of intense reflections in the refinements.[32] The highest and lowest peaks in the final difference Fourier map had electron densities of 0.47 and −0.38 e/Å^3, respectively.

Acknowledgment. This work was supported by the Director, Office of Energy Research, Office of Basic Energy Sciences, Chemical Sciences Division of the U.S. Department of Energy under Contract No. DE-ACO3-76DF00098. We also thank the National Science Foundation for a predoctoral fellowship to M.E.S. and Wayne Lukens and Marc Weydert for discussions.

Supporting Information Available: A complete listing of bond distances, angles, anisotropic thermal parameters, and positional parameters (14 pages). See any current masthead page for ordering and Internet access instructions.

JA953873F